Absence of endolymphatic sac ion transport proteins in large vestibular aqueduct syndrome - A human temporal bone study

Eckhard, Andreas H ; Bächinger, David ; Nadol, Joseph B

Abstract: Hypothesis: Epithelial ion transport pathologies of the endolymphatic sac (ES) are associated with large vestibular aqueduct syndrome (LVAS). Background: LVAS is defined by the pathognomonic features of a widened bony vestibular aqueduct (VA) and an enlarged ES. The underlying cause of its associated cochleovestibular symptoms remains elusive. Disturbances in epithelial ion transport in the enlarged ES, affecting inner ear fluid regulation, were proposed as a possible pathophysiology. However, although respective epithelial ion transport pathologies have been demonstrated in the enlarged ES from transgenic LVAS mouse models, these pathologies have not been investigated in human LVAS cases. Methods: Histological and immunohistochemical analysis of the enlarged ES epithelium in postmortem temporal bones from two individuals with a clinical diagnosis of LVAS. Results: The enlarged ES epithelium demonstrated an overall atypical epithelial differentiation and a lack of the immunolocalization of signature ion transport proteins. Notably, in both cases, a rudimentary branch of the ES with a typically differentiated ES epithelium was present. Conclusions: The described cellular and molecular pathologies of the enlarged ES in humans provide evidence of epithelial transport pathology as one potential cause of cochleovestibular symptoms in LVAS. The present findings also emphasize the clinical relevance of already established LVAS mouse models.

DOI: https://doi.org/10.1097/mao.0000000000002832

Absence of Endolymphatic Sac Ion Transport Proteins in Large Vestibular Aqueduct Syndrome—A Human Temporal Bone Study

*†Andreas H. Eckhard, *†David Bächinger, and ‡§Joseph B. Nadol Jr.

*Department of Otorhinolaryngology, Head and Neck Surgery, University Hospital Zurich; †University of Zurich, Zurich, Switzerland; ‡Otopathology Laboratory, Department of Otolaryngology, Massachusetts Eye and Ear Infirmary; and §Department of Otolaryngology, Harvard Medical School, Boston, Massachusetts, USA

Hypothesis: Epithelial ion transport pathologies of the endolymphatic sac (ES) are associated with large vestibular aqueduct syndrome (LVAS).
Background: LVAS is defined by the pathognomonic features of a widened bony vestibular aqueduct (VA) and an enlarged ES. The underlying cause of its associated cochleovestibular symptoms remains elusive. Disturbances in epithelial ion transport in the enlarged ES, affecting inner ear fluid regulation, were proposed as a possible pathophysiology. However, although respective epithelial ion transport pathologies have been demonstrated in the enlarged ES from transgenic LVAS mouse models, these pathologies have not been investigated in human LVAS cases.
Methods: Histological and immunohistochemical analysis of the enlarged ES epithelium in postmortem temporal bones from two individuals with a clinical diagnosis of LVAS.
Results: The enlarged ES epithelium demonstrated an overall atypical epithelial differentiation and a lack of the immunolocalization of signature ion transport proteins. Notably, in both cases, a rudimentary branch of the ES with a typically differentiated ES epithelium was present.
Conclusions: The described cellular and molecular pathologies of the enlarged ES in humans provide evidence of epithelial transport pathology as one potential cause of cochleovestibular symptoms in LVAS. The present findings also emphasize the clinical relevance of already established LVAS mouse models. **Key Words:** Endolymphatic hydrops—Enlarged vestibular aqueduct—Epithelial sodium channel—Menière's disease—Pendrin.

Otol Neurotol **41:**xxx–xxx, 2020.

Large vestibular aqueduct syndrome (LVAS) is characterized by the pathognomonic features of a widened bony vestibular aqueduct (VA) and an enlarged endolymphatic sac (ES) (1,2). Clinically, LVAS usually manifests as sensorineural, mixed, or, rarely, purely conductive hearing loss in early childhood and often exhibits a fluctuating and progressive course (reviewed in (3–5)). Concomitant vestibular symptoms ranging from chronic disequilibrium to an episodic Menière's-like symptom complex can occur (6–9). The most frequent causes of LVAS (10) are considered mutations in the *SLC26A4* gene (11,12), which encodes the anion exchanger pendrin (13). In the human and murine inner ear, pendrin is expressed by nonsensory cells in the cochlea, the vestibular labyrinth, and the ES epithelium (14,15). Notably, a lack of pendrin expression in the ES (ES-specific pendrin knockout mice)—but not in the cochleovestibular epithelia—leads to the development of an inner ear phenotype that resembles LVAS (reviewed in (16)). The pathophysiology that underlies this LVAS phenotype in mice presumably involves a lack of pendrin-dependent chloride and bicarbonate transport, as well as secondarily diminished functions of the epithelial sodium channel (ENaC (17)) and other ion transport proteins (17–20). Although pendrin (21) and ENaC (22) are present in the normal human ES epithelium, the enlarged ES epithelium from LVAS patients has thus far not been investigated for potential ion transport pathologies. Here, we analyzed the epithelial morphology and the immunohistochemical localization patterns of the three ENaC subunits in the enlarged ES on histologically processed temporal bone sections from two individuals with a clinical diagnosis of LVAS. The results shed light on the molecular pathologies in the human enlarged ES epithelium and draw parallels to the molecular ion transport pathologies in LVAS mouse models.

Address correspondence and reprint requests to Andreas H. Eckhard, M.D., Department of Otorhinolaryngology, University Hospital Zurich, Frauenklinikstrasse 24, 8091 Zurich, Switzerland; E-mail: AndreasHeinrich.Eckhard@usz.ch

The study was supported by a grant from the Zürcher Stiftung für das Hören. D.B. is supported by a national MD-PhD scholarship from the Swiss National Science Foundation (SNSF). A.H.E. is supported by a career development grant from the University of Zurich.

The authors disclose no conflicts of interest.

DOI: 10.1097/MAO.0000000000002832

METHODS

Human Temporal Bone Cases

The database of the human temporal bone (TB) collection at the Massachusetts Eye and Ear Infirmary was searched with the key words ''enlarged/large vestibular aqueduct/endolymphatic sac.'' The search retrieved a total of eight cases. Two of those cases (only one TB specimen was available from each case) were included in the study because their enlarged VA and ES were completely preserved and without any artifactual damage. Computed tomography (CT) scans of the extracted specimens were acquired before histological processing using dedicated standard protocols for TB imaging. The specimens were histologically processed according to previously described methods (23). The temporal bone pathology in case #2 was recently published (24), excluding the ES pathologies described here.

Morphometry of the VA

In each specimen, the diameter of the VA in the axial plane was determined by measuring the maximum distance between the two bony lips that form the operculum on CT images and histological sections from corresponding images/section planes, according to (25,26).

Immunohistochemistry

Celloidin sections were mounted on microscope slides, and the celloidin was removed according to methods described previously (27). The sections were blocked in 5% normal horse serum (NHS) diluted in phosphate-buffered saline (PBS) and incubated overnight with primary antibodies that were raised in rabbit and directed against the α- (αENaC), β- (βENaC), and γ- (γENaC) subunits of the ENaC (a gift from Prof. J. Loffing, University of Zurich). The sections were then incubated with biotinylated secondary antibodies that were raised in donkey and directed against rabbit IgG for 1 hour, followed by the application of an avidin–biotin complex reagent (Jackson ImmunoResearch, West Grove, PA) for 1 hour, an amplification step that included incubation with biotinylated tyramine for 10 minutes, and incubation with avidin–biotin complex reagent for 30 minutes. Then, all sections were incubated in diaminobenzidine/hydrogen peroxide in PBS supplemented with 4% 3,3′-diaminobenzidine (Sigma, St. Louis, MO) for 2 to 10 minutes. The slides were then dehydrated in an ascending ethanol series, cleared with xylenes, and mounted for microscopic analysis. All primary and secondary antibodies were diluted in 1% NHS/PBS. All incubation steps were performed at RT and followed by two 5 minutes washes in PBS.

Microscopic Analysis

Images were acquired using an ACCU-Scope AU-600-HD Excelis HD High Definition Color Microscopy Camera with Live HDMI video (Accu Scope Inc., New York, NY) and processed with CorelDraw software (Corel Inc., Ottawa, Canada).

RESULTS

Human LVAS Cases

Case #1 (Table 1) was a 66-year-old male with a clinical history of early-onset (age 8) bilateral sensorineural hearing loss, which, at age 44, had progressed to severe levels. Before left cochlear implantation at age 47, a CT scan demonstrated bilateral Mondini deformities and bilateral large VAs. Postoperative fluctuations in hearing and increased tinnitus were noted in the implanted left ear, as well as at least two occasions of nausea and dizziness. Retrospectively, the patient reported some fluctuation in hearing and tinnitus earlier in life. A tentative diagnosis of Menière's syndrome was made. At age 64, he underwent cochlear implantation in the right inner ear. Two years later (age 66), the patient developed bacterial meningitis, and the right cochlear implant was removed in a canal wall-down mastoidectomy procedure. He died a month later following a cardiac catheterization procedure for coronary heart disease. The histopathological findings from the right TB specimen included a shortened cochlear duct (1 1/4 turns) with malformation of the apical and middle turns, consistent with the radiographic diagnosis of incomplete partition type 2 (hypoplastic modiolus, scala communis in the apical turn (28)). The cochlear and vestibular spaces were almost entirely filled with mature granulation tissue. The cochlear implant track, which reached from the cochleostomy site well into the scala vestibuli, was lined with granulation tissue, cellular debris, and a few foreign body giant cells. The scala tympani in the basal turn was largely filled with new bone. CT imaging (Fig. 1A) and histological examination of the right TB (Fig. 1, B and B') demonstrated a widened VA with an axial diameter of 1.7 mm, which was more than double the diameter of the posterior semicircular canal (pSCC; 0.6 mm), thus matching the different pathomorphological criteria of an enlarged VA (e.g., opercular width >1.5 mm (25,26,29)).

Case #2 (Table 1) was an 18-year-old man diagnosed with Kleefstra syndrome (microdeletion on chromosome

TABLE 1. *Clinical and histopathological features of the two LVAS cases*

Feature	Case #1	Case #2
Sex	Male	Male
Age at death (years)	66	18
Cause of death	Cerebral hemorrhage	Cardiomyopathy/ cardiac failure
Hearing loss		
Age at onset (years)	8	n.k.
Type	Sensorineural, fluctuating	Mixed
Affected side	Bilateral	Bilateral
Tinnitus	Yes	n.k.
Vestibular symptoms	Episodic dizziness	n.k.
Available TB specimen	Right	Left
Post mortem time (hours)	4	38.5
VA diameter (mm[a])	2.3	3.5
Other histopathologies		
Cochlea	Mondini dysplasia	
Vestibular portion		

[a]As measured in histological sections.
n.k. indicates not known; TB, temporal bone.

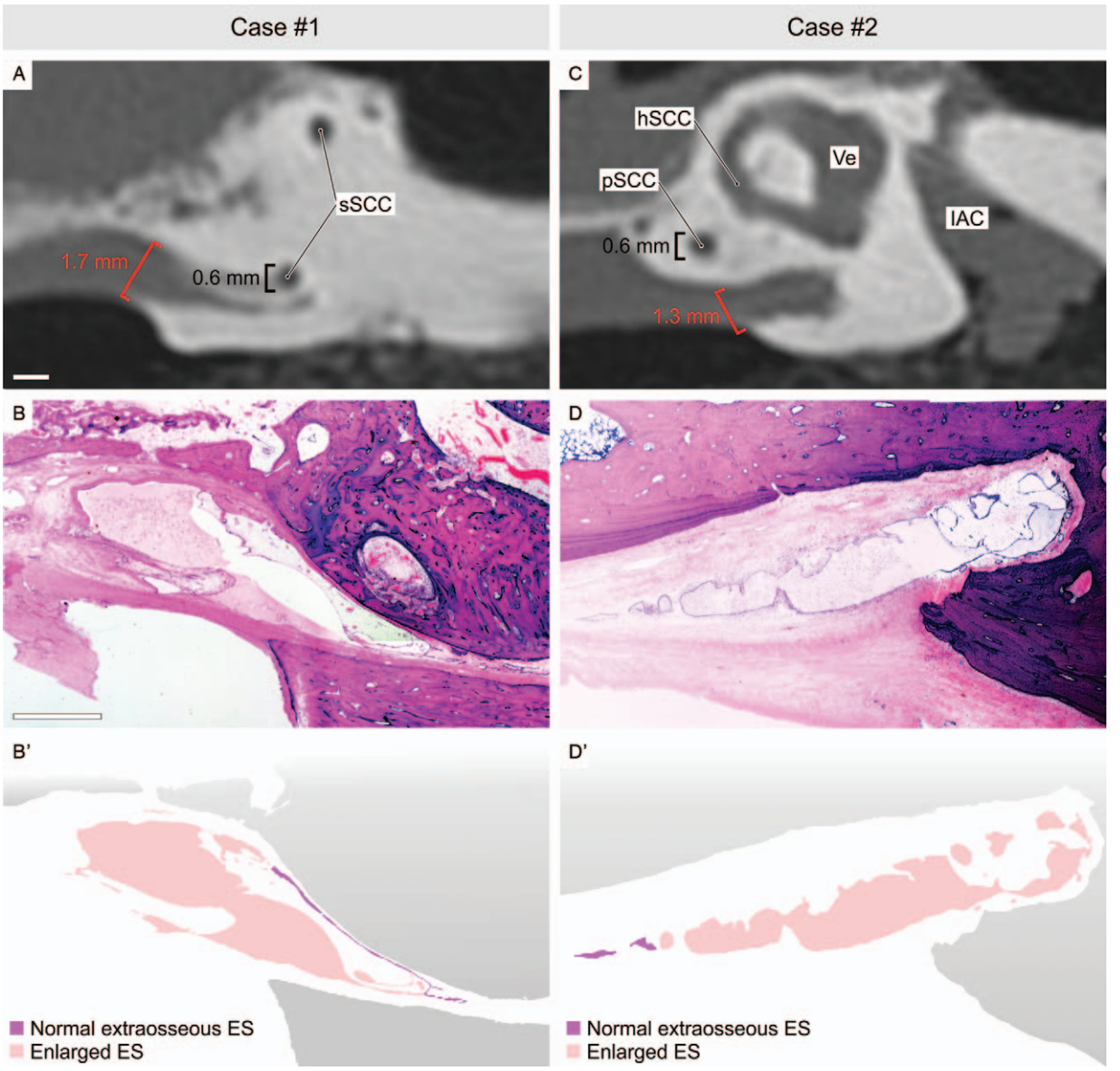

FIG. 1. Computed tomography (CT) images (axial plane) showing the enlarged VA areas from case #1 (*A*) and case #2 (*C*). sSCC indicates superior semicircular canal; hSCC, horizontal semicircular canal; pSCC, posterior semicircular canal; Ve, vestibule; IAC, internal auditory canal. Hematoxylin-eosin-stained sections of the opercular region and ES as well as schematized histological structures from case #1 (*B*, *B*') and case #2 (*D*, *D*'). Measurements of the VA diameter at the operculum ("opercular width") were performed according to previously published methods (25,26) (1.7 mm in (*A*), 1.3 mm in (*C*)). The maximum radial diameter of the pSCC in both cases was determined to be 0.6 mm (*A*, *C*; in (*A*) only the sSCC is shown, the measurements of the pSCC were performed in a different section plane). Scale bars: 1 mm.

9q34.3 (30,31)). His clinical symptoms included bilateral mixed hearing loss, microcephaly, typical facial dysmorphism, bilateral optic nerve hypoplasia with blindness, diffuse hypotonia, dilated cardiomyopathy, chronic lung disease secondary to microaspiration, and scoliosis. After aortic valve replacement, he suffered from deteriorating cardiac function. At age 18, he was transferred to a hospital with severe cardiac dysfunction and died after unsuccessful resuscitation efforts. On histopathological examination, the middle ear and mastoid appeared unremarkable, except for a thickened posterior crus of the stapes. In the cochlea, the modiolus was dysmorphic and absent in the apical turn, which presented as scala communis, indicating an incomplete partition type 2 (28). No signs of endolymphatic hydrops were visible in the cochlea or vestibular portions. The number of spiral ganglion cells in Rosenthal's canal and the associated dendrites in the spiral lamina were markedly reduced (approximately 34% of that determined by previous quantifications in age-matched controls). No hair cells were present in the lower basal turn of the organ of Corti. The vestibular system also exhibited dysmorphic

changes, including dislocation of the cristae of the superior and lateral semicircular canals and macula utriculi in the anterior/superior aspect of the vestibule. CT imaging (Fig. 1C) and histological examination of the left TB (Fig. 1D and D') demonstrated that the VA had an opercular width (1.3 mm) more than double the diameter of the posterior semicircular canal (0.6 mm); thus, matching at least one criterion for an enlarged VA (29).

Atypical Epithelial Cell Morphology in the Enlarged ES

In both cases, the ES, particularly the extraosseous ES (eES) portion, which stretches from the operculum into the dura of the posterior cranial fossa, demonstrated a single, cyst-like, enlarged lumen (Fig. 1, B and D). This luminal space was partially filled with cells and an eosinophilic amorphous substance. Its epithelial lining consisted predominantly of an atypical squamous epithelium with interspersed patches of cuboidal or columnar epithelial cells (Fig. 2,A and E). Notably, in both cases, a small branch of the eES presented a normal-sized lumen, the epithelium of which consisted of typical uniform, cuboidal cells (Fig. 2, C and G).

Absence of Signature Ion Transport Proteins in the Enlarged ES

Immunolabeling for the αENaC, βENaC, and γENaC subunits was performed on celloidin-embedded sections from the two LVAS cases. The epithelium of the enlarged eES was virtually devoid of any specific immunolabeling for the three ENaC subunits (Fig. 2, B and B'' (case #1), and F–F'' (case #2)). In contrast, the portion of the eES branch, which exhibited typical homogenous cuboidal epithelium and normal sized lumen (see the previous paragraph), demonstrated strong immunolabeling for all ENaC subunits in many cells (Fig. 2D–D'' (case #1), and H–H'' (case #2)). The immunolabeling signals for γENaC and βENaC were often polarized toward the apical membrane domain, while αENaC immunolabeling was homogenous throughout the cytoplasm. These immunolabeling patterns are consistent with those previously described in the normal human eES (32). As an internal positive control, immunolabeling for all three ENaC subunits was also detected in the apical cell membranes and the cytoplasm of the middle ear epithelium (data not shown (33)).

Inflammatory Cell Infiltration in the Enlarged ES

In the dural tissue surrounding the enlarged eES, large numbers of immune cells, predominantly polymorphonuclear leukocytes and macrophages, were found in both cases (Fig. 3,A and B). These inflammatory cells accumulated in scattered focal areas in the subepithelial space, appeared to transmigrate across the ES epithelial border (inlay, Fig. 3B), and presented in unusual density in the luminal space. Large numbers of luminal and perisaccular cells were identified as macrophages based on their positive immunolabeling for calcium-binding adapter molecule 1 (IBA1; Fig. 3, C and D). IBA1 immunolabeling in a normal eES (adult control case) is provided for comparison (Fig. 3E). Although the history of cochlear implantation and meningitis in case #1 may constitute a confounder in the present analysis, very similar proinflammatory immune cell patterns were identified in case #2, despite the lack of such confounding factors according to the clinical records.

On note, the histo- and immunopathologies in the enlarged ES from a third LVAS case were recently presented at the Otopathology conference, hosted at the Massachusetts Eye and Ear (Boston, MA). A webcast of this presentation is available online (http://otopathologylaboratory.org/educational-resources/webcasts/?). The findings in this third case were very similar to those reported here for cases #1 and #2, and further support our conclusions (see Discussion section).

DISCUSSION

The most common causes of LVAS are mutations in the *SLC26A4* gene, which encodes the chloride (Cl^-)/bicarbonate (HCO_3^-) exchanger pendrin; these mutations are found in up to 90% of patients (34–36). Pendrin is expressed in different cell types in the human and murine inner ear, including spiral prominence cells and outer sulcus cells in the cochlear spiral ligament (15,37), transitional cells in the utricle, saccule and ampullae (14,37), and mitochondria-rich epithelial cells in the ES (14,15).

Among the inner ear epithelia, the ES is a particularly critical site for pendrin function. Targeted disruption of pendrin gene expression in the ES of *Foxi1* knockout ($Foxi1^{-/-}$) mice causes an inner ear phenotype that resembles LVAS in humans (38). A key pathogenetic event in the pendrin-deficient murine inner ear is a reduction in endolymph pH (acidification) due to the loss of pendrin-mediated HCO_3^- transport (18). Endolymph acidification diminishes ENaC gene expression in the inner ear epithelia (19), and probably inhibits the resorption of endolymphatic Na^+. This effect is thought to cause sodium chloride (NaCl) retention and osmotic volume expansion of the endolymphatic fluid compartment, which ultimately determine the pathomorphological features of the LVAS phenotype, i.e., enlargement of the ES and VA and the development of cochleovestibular hydrops (19,20). Moreover, endolymph acidification may also inhibit the pH-sensitive transient receptor potential subfamily V (TRPV) members TRPV5 and TRPV6, which are also expressed in different epithelial cell types in the inner ear, including the endolymphatic sac (39–42). Inhibition of TRPV5 and TRPV6 may explain the pathological increase in endolymphatic Ca^{2+} (40), which is thought to disturb hair cell function (43,44), and thus may play an important role in the pathogenesis of cochleovestibular symptoms in LVAS mouse models (40).

Here, we demonstrate the overall absence of immunolabeling for all three ENaC subunits in the enlarged human ES. This finding clearly contrasts the presence of

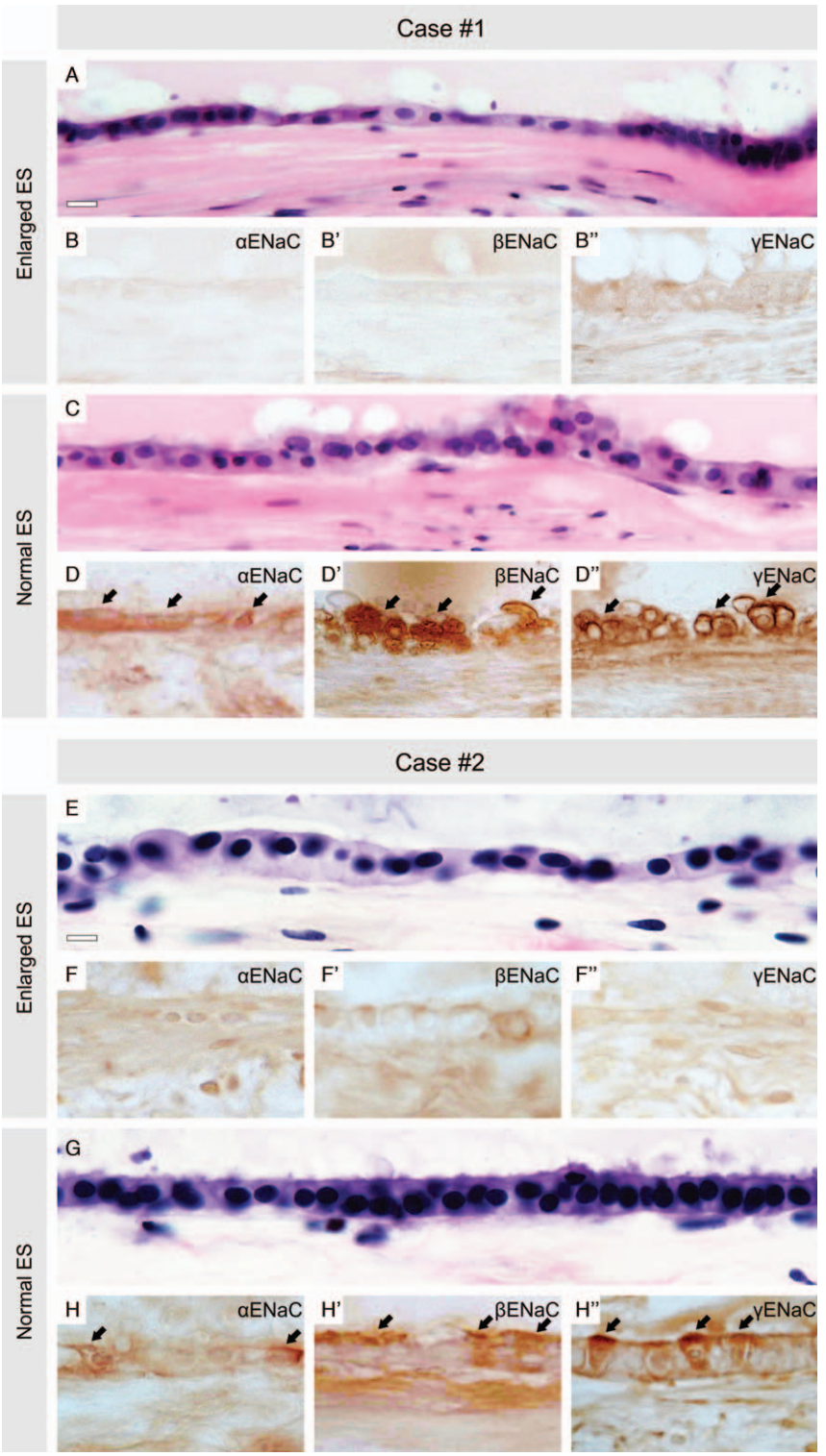

FIG. 2. Representative epithelial morphology in the enlarged ES (*A* and *E*) and the rudimentary "normal" portion of the eES (*C* and *G*) in cases #1 and #2. Immunolabeling of α-, b-, and γENaC in enlarged ES (*B–B*", *F–F*") and "normal" eES (*D–D*", *H–H*') portions from both cases (black *arrows* indicate ENaC-labeled epithelial cells). Scale bars: 10 μm.

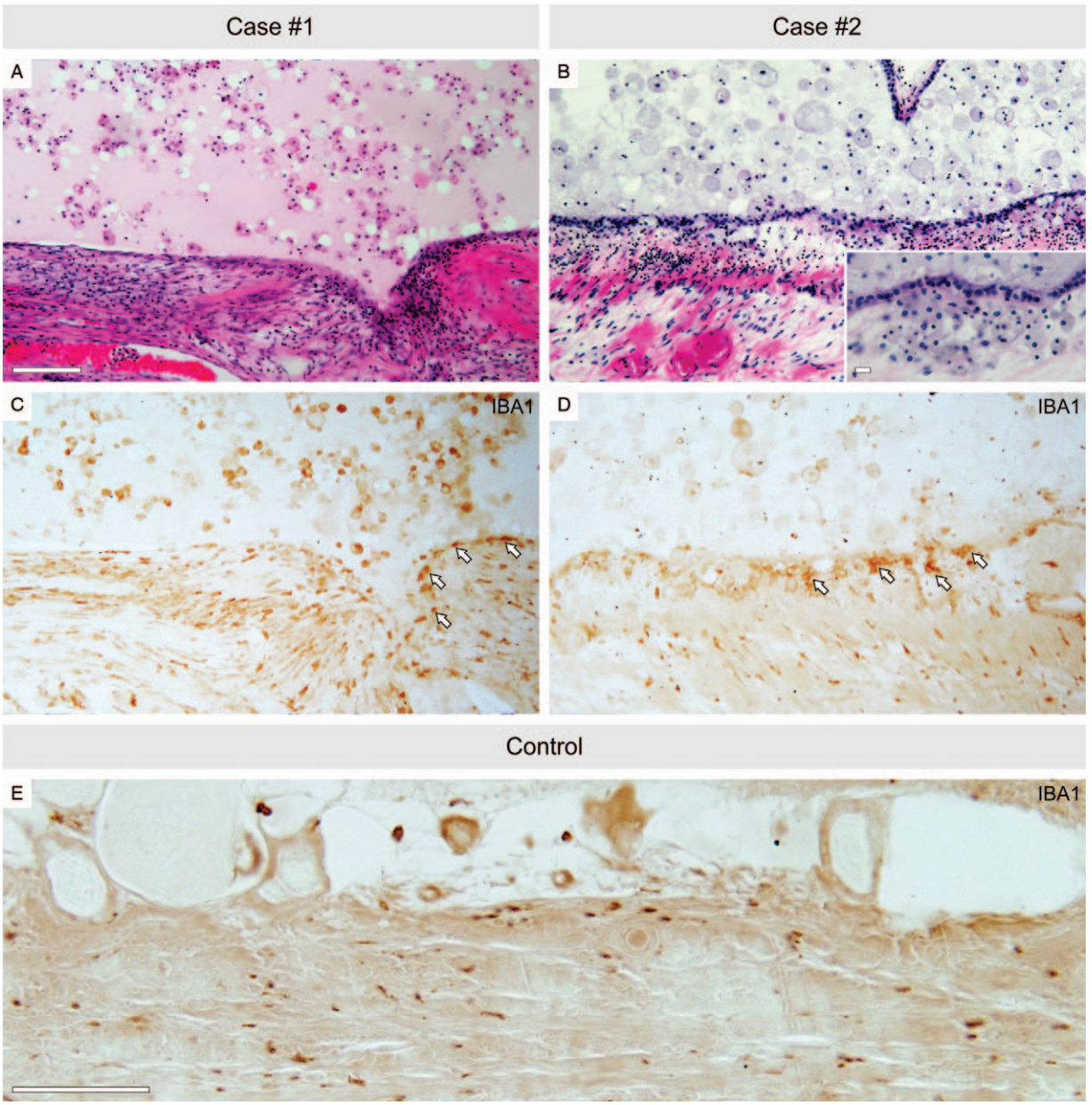

FIG. 3. Massive accumulation of inflammatory cells at the epithelial border of enlarged ES portions in cases #1 (*A*) and #2 (*B*). IBA1 immunolabeling identified many luminal and subepithelial cells as macrophages, particularly those that appear to transmigrate across the ES epithelial barrier (*arrows* in (*C*) (case #1) and (*D*) (case #2)). IBA1 immunolabeling in the ES from a normal (no history of otologic disease) control case (*E*). Scale bars: 100 μm; inset (*B*), 10 μm.

abundant ENaC in the normal human eES described previously (32). However, it is consistent with diminished ENaC expression in the inner ears from LVAS mouse models (see the previous paragraph). The cause of the lack of ENaC in the enlarged human ES remains unknown from our study but could be either a primary (its absent expression in an abnormally differentiated enlarged ES epithelium) or secondary (expression down-regulation caused by altered endolymph fluid composition, e.g., acidification) pathology. Finally, the presence of a variably sized, rudimentary eES portion with a typical epithelial morphology, strong ENaC immunolabeling, and presumably normal ion transport capabilities, may affect the manifestation and progression of cochleovestibular dysfunction in LVAS, and thus help to explain the heterogeneous clinical presentations among patients.

In summary, the present findings suggest a common underlying epithelial transport pathology in the enlarged ES epithelium that affects endolymphatic osmoregulation and volume regulation in both animal models and LVAS patients.

Notably, in a recent histopathological study on Menière's disease, we described two epithelial pathologies—idiopathic epithelial degeneration and developmental hypoplasia—both of which affect the eES and are associated with the loss of eES-specific ion transport proteins, including ENaC (32). Apart from their different sizes, the hypoplastic ES of Menière's patients (32,45) and enlarged ES in LVAS patients have strikingly similar hallmark pathological features: 1) a cyst-like (single lumen) ES, 2) mostly squamous-like epithelium, 3) markedly reduced (absent) ENaC protein abundance, and 4) abnormal morphology of the bony VA (widened in LVAS, narrowed in Menière's disease). Thus, although different etiologies may lead to enlargement or hypoplasia of the ES, the pathophysiological consequences may be very similar, which would explain the Menière's-like clinical features that are often reported in many LVAS patients (such as case #1 in the present study); these features include cochleovestibular hydrops ((46,47); not conclusively analyzed in the two present cases; see Results section), fluctuating progressive sensorineural hearing loss, and episodic dizziness/vertigo (2,3,7,48). As a side note, the air-bone gap commonly observed in LVAS patients is best explained by a pathologic third window effect of the widened VA (49). The, often rapid, progressive sensorineural hearing loss is most likely due to the degeneration of neurosensory structures, which may be a consequence of, e.g., the here-proposed ES dysfunction or other ion transport pathologies within the inner ear, or the structural cochlear partitioning defect, or a combination of these pathologies.

An ambiguous finding of the present study is the massive infiltration of immune cells, mostly $IBA1^+$ macrophages, in the ES luminal space, and the perisaccular region. This proinflammatory pattern is unlikely to be a postmortem artifact since, at least in case #1, the time from death to formalin fixation was as short as 4 hours (38.5 h in case #2). Some possible causes that could explain this local immune cell recruitment include a reduced pH (acidification (50)) and an elevated Na^+ concentration (51) in the enlarged ES; thus, this finding may be directly linked to the impaired ion transport capabilities of the ES epithelium.

A limitation of the present study is the unknown *SLC26A4* genotype in both cases, which raises the question of whether the reported findings can be generalized to a broader LVAS population. However, that very similar (immuno)histopathologies were present in both cases, although they represented categorically different forms of LVAS—nonsyndromic (case #1) and syndromic (case #2 associated with Kleefstra syndrome) —argues for the broad relevance of the present findings. Moreover, in addition to ENaC, the enlarged ES epithelium may lack other crucial ion transport proteins, which were not analyzed in the present study, mainly due to the impediment of the limited antigenicity of the archival celloidin-embedded tissue sections.

In conclusion, the present findings support the concept of an epithelial transport pathology in the enlarged ES as an etiopathogenetic factor for LVAS. Furthermore, we propose that certain cellular and molecular ES pathologies are shared between patients with LVAS and those with Menière's disease (endotype with ES hypoplasia), which may explain the similar, and often overlapping, clinical features in these two patient groups. In both LVAS and Menière's disease, the bony abnormalities of the VA associated with LVAS (VA widening) and Menière's disease (VA hypoplasia) may be regarded as ''fossil-like records'' (52) of the underlying epithelial pathologies, the former of which serve as radiological surrogate markers (48,53). Lastly, the present findings draw parallels to the pathophysiology of LVAS mouse models and thereby help validate those models as important research tools in which to study the human condition.

Acknowledgments: The authors are grateful for the exceptional technical expertise of Barbara Burgess, Diane Jones, MengYu Zhu, and Jennifer O'Malley in preparing the human temporal bone specimens. The authors thank Prof. J. Loffing (Institute of Anatomy, University of Zurich, Switzerland) for providing the ENaC antibodies.

REFERENCES

1. Beal DD, Davey PR, Lindsay JR. Inner ear pathology of congenital deafness. *Arch Otolaryngol* 1967;85:134–42.
2. Valvassori GE, Clemis JD. The large vestibular aqueduct syndrome. *Laryngoscope* 1978;88:723–8.
3. Govaerts PJ, Casselman J, Daemers K, De Ceulaer G, Somers T, Offeciers FE. Audiological findings in large vestibular aqueduct syndrome. *Int J Pediatr Otorhinolaryngol* 1999;51:. 157–64.
4. Berrettini S, Forli F, Bogazzi F, et al. Large vestibular aqueduct syndrome: Audiological, radiological, clinical, and genetic features. *Am J Otolaryngol* 2005;26:363–71.
5. Gopen Q, Zhou G, Whittemore K, Kenna M. Enlarged vestibular aqueduct: Review of controversial aspects. *Laryngoscope* 2011;121: 1971–8.
6. Valvassori GE, Naunton RF, Lindsay JR. Inner ear anomalies: Clinical and histopathological considerations. *Ann Otol Rhinol Laryngol* 1969;78:929–38.
7. Schessel DA, Nedzelski JM. Presentation of large vestibular aqueduct syndrome to a dizziness unit. *J Otolaryngol* 1992;21:265–9.
8. Okumura T, Takahashi H, Honjo I, et al. Vestibular function in patients with a large vestibular aqueduct. *Acta Otolaryngol* 1995;115:323–6.
9. Grimmer JF, Hedlund G. Vestibular symptoms in children with enlarged vestibular aqueduct anomaly. *Int J Pediatr Otorhinolaryngol* 2007;71:275–82.
10. Albert S, Blons H, Jonard L, et al. SLC26A4 gene is frequently involved in nonsyndromic hearing impairment with enlarged vestibular aqueduct in Caucasian populations. *Eur J Hum Genet* 2006;14:773–9.
11. Li XC, Everett LA, Lalwani AK, et al. A mutation in PDS causes non-syndromic recessive deafness. *Nat Genet* 1998;18:215–7.
12. Usami SI, Abe S, Weston MD, Shinkawa H, Van Camp G, Kimberling WJ. Non-syndromic hearing loss associated with enlarged vestibular aqueduct is caused by PDS mutations. *Hum Genet* 1999;104:188–92.
13. Scott DA, Wang R, Kreman TM, Sheffield VC, Karniski LP. The Pendred syndrome gene encodes a chloride-iodide transport protein. *Nat Genet* 1999;21:440–3.
14. Royaux IE, Belyantseva IA, Wu T, et al. Localization and functional studies of pendrin in the mouse inner ear provide insight about the etiology of deafness in Pendred syndrome. *J Assoc Res Otolaryngol* 2003;4:394–404.

15. Wangemann P, Itza EM, Albrecht B, et al. Loss of KCNJ10 protein expression abolishes endocochlear potential and causes deafness in Pendred syndrome mouse model. *BMC Med* 2004;2:30.
16. Wangemann P, Griffith AJl. Mouse models reveal the role of pendrin in the inner ear. In: Dossena S, Paulmichl M, editors. *The Role of Pendrin in Health and Disease*. Springer: Cham; 2017.
17. Kim BG, Kim JY, Kim HN, et al. Developmental changes of ENaC expression and function in the inner ear of pendrin knock-out mice as a perspective on the development of endolymphatic hydrops. *PLoS One* 2014;9:e95730.
18. Wangemann P, Nakaya K, Wu T, et al. Loss of cochlear HCO3- secretion causes deafness via endolymphatic acidification and inhibition of Ca2+ reabsorption in a Pendred syndrome mouse model. *Am J Physiol Renal Physiol* 2007;292:F1345–53.
19. Kim HM, Wangemann P. Epithelial cell stretching and luminal acidification lead to a retarded development of stria vascularis and deafness in mice lacking pendrin. *PLoS One* 2011;6:e17949.
20. Li X, Zhou F, Marcus DC, Wangemann P. Endolymphatic Na+ and K+ concentrations during cochlear growth and enlargement in mice lacking *Slc26a4*/pendrin. *PLoS One* 2013;8:e65977.
21. Møller MN, Kirkeby S, Vikeså J, Nielsen FC, Cayé-Thomasen P. Gene expression in the human endolymphatic sac: The solute carrier molecules in endolymphatic fluid homeostasis. *Otol Neurotol* 2015;36:915–22.
22. Kim SH, Park HY, Choi HS, Chung HP, Choi JY. Functional and molecular expression of epithelial sodium channels in cultured human endolymphatic sac epithelial cells. *Otol Neurotol* 2009;30:529–34.
23. Merchant SN, Nadol JB. *Schuknecht's Pathology of the Ear*, 3rd ed. People's Medical Pub House-USA; Stamford, CT. 2010.
24. Okayasu T, Quesnel AM, Reinshagen KL, Nadol JB Jr. Otopathology in Kleefstra syndrome: A case report. *Laryngoscope* 2019. Online ahead of print.
25. Levenson MJ, Parisier SC, Jacobs M, Edelstein DR. The large vestibular aqueduct syndrome in children. A review of 12 cases and the description of a new clinical entity. *Arch Otolaryngol Head Neck Surg* 1989;115:54–8.
26. Vijayasekaran S, Halsted MJ, Boston M, et al. When is the vestibular aqueduct enlarged? A statistical analysis of the normative distribution of vestibular aqueduct size. *Am J Neuroradiol* 2007;28:1133–8.
27. O'Malley JT, Burgess BJ, Jones DD, Adams JC, Merchant SN. Techniques of celloidin removal from temporal bone sections. *Ann Otol Rhinol Laryngol* 2009;118:435–441.
28. Sennaroglu L, Saatci I. A new classification for cochleovestibular malformations. *Laryngoscope* 2002;112:2230–41.
29. Weissman JL. Hearing loss. *Radiology* 1996;199:593–611.
30. Schimmenti LA, Berry SA, Tuchman M, Hirsch B. Infant with multiple congenital anomalies and deletion (9)(q34.3). *Am J Med Genet* 1994;51:140–2.
31. Kleefstra T, Brunner HG, Amiel J, et al. Loss-of-function mutations in Euchromatin histone methyl transferase 1 (EHMT1) cause the 9q34 subtelomeric deletion syndrome. *Am J Hum Genet* 2006;79:370–7.
32. Eckhard AH, Zhu M, O'Malley JT, et al. Inner ear pathologies impair sodium-regulated ion transport in Meniere's disease. *Acta Neuropathol* 2019;137:343–57.
33. Choi JY, Son EJ, Kim JL, et al. ENaC- and CFTR-dependent ion and fluid transport in human middle ear epithelial cells. *Hear Res* 2006;211:26–32.
34. Reardon W, OMahoney CF, Trembath R, Jan H, Phelps PD. Enlarged vestibular aqueduct: A radiological marker of Pendred syndrome, and mutation of the PDS gene. *QJM* 2000;93:99–104.
35. Tsukamoto K, Suzuki H, Harada D, Namba A, Abe S, Usami SI. Distribution and frequencies of PDS (SLC26A4) mutations in Pendred syndrome and nonsyndromic hearing loss associated with enlarged vestibular aqueduct: A unique spectrum of mutations in Japanese. *Eur J Hum Genet* 2003;11:916–22.
36. Liu Y, Wang L, Feng Y, et al. A new genetic diagnostic for enlarged vestibular aqueduct based on next-generation sequencing. *PLoS One* 2016;11:e0168508.
37. Everett LA, Morsli H, Wu DK, Green ED. Expression pattern of the mouse ortholog of the Pendred's syndrome gene (Pds) suggests a key role for pendrin in the inner ear. *Proc Natl Acad Sci U S A* 1999;96:9727–32.
38. Hulander M. Lack of pendrin expression leads to deafness and expansion of the endolymphatic compartment in inner ears of Foxi1 null mutant mice. *Development* 2003;130:2013–25.
39. Yeh B Il, Yung KK, Jabbar W, Huang CL. Conformational changes of pore helix coupled to gating of TRPV5 by protons. *EMBO J* 2005;24:3224–34.
40. Nakaya K, Harbidge DG, Wangemann P, et al. Lack of pendrin HCO3- transport elevates vestibular endolymphatic [Ca2+] by inhibition of acid-sensitive TRPV5 and TRPV6 channels. *Am J Physiol Renal Physiol* 2007;292:F1314–21.
41. Yamauchi D, Nakaya K, Raveendran NN, et al. Expression of epithelial calcium transport system in rat cochlea and vestibular labyrinth. *BMC Physiol* 2010;10:1.
42. Bächinger D, Egli H, Goosmann MM, Monge Naldi A, Loffing J, Eckhard AH. Immunolocalization of the calcium sensing receptor (CaSR) and calcium transport proteins indicate a calciostatic function of the murine endolymphatic sac. *Cell Tissue Res* 2019;378:163–73.
43. Tanaka Y, Asunuma A, Yanagisawa K. Potentials of outer hair cells and their membrane properties in cationic environments. *Hear Res* 1980;2:431–8.
44. Ohmori H. Mechano-electrical transduction currents in isolated vestibular hair cells of the chick. *J Physiol* 1985;359:189–217.
45. Bächinger D, Brühlmann C, Honegger T, et al. Endotype-phenotype patterns in Meniere's disease based on gadolinium-enhanced MRI of the vestibular aqueduct. *Front Neurol* 2019;10:303.
46. Spiegel JH, Lalwani AK. Large vestibular aqueduct syndrome and endolymphatic hydrops: Two presentations of a common primary inner-ear dysfunction? *J Laryngol Otol* 2009;123:919–21.
47. Ralli M, Nola G, Sparvoli L, Ralli G. Unilateral enlarged vestibular aqueduct syndrome and bilateral endolymphatic hydrops. *Case Rep Otolaryngol* 2017;2017:6195317.
48. Griffith AJ, Arts A, Downs C, et al. Familial large vestibular aqueduct syndrome. *Laryngoscope* 1996;106:960–5.
49. Merchant SN, Nakajima HH, Halpin C, et al. Clinical investigation and mechanism of air-bone gaps in large vestibular aqueduct syndrome. *Ann Otol Rhinol Laryngol* 2007;116:532–41.
50. Riemann A, Wußling H, Loppnow H, Fu H, Reime S, Thews O. Acidosis differently modulates the inflammatory program in monocytes and macrophages. *Biochim Biophys Acta* 2016;1862:72–81.
51. Hucke S, Eschborn M, Liebmann M, et al. Sodium chloride promotes pro-inflammatory macrophage polarization thereby aggravating CNS autoimmunity. *J Autoimmun* 2016;67:90–101.
52. Li X, Sanneman JD, Harbidge DG, et al. SLC26A4 targeted to the endolymphatic sac rescues hearing and balance in Slc26a4 mutant mice. *PLoS Genet* 2013;9:e1003641.
53. Bächinger D, Luu N-NN, Kempfle JS, et al. Vestibular aqueduct morphology correlates with endolymphatic sac pathologies in Menière's disease: A correlative histology and computed tomography study. *Otol Neurotol* 2019;40:e548–e555.